

First-difference fluctuations and the complexity of simple population models exhibiting chaos

Octavio Miramontes^{a,*}, Eliane Ceccon^b

^a*Departamento de Sistemas Complejos, Instituto de Física, Universidad Nacional Autónoma de México, México 01000, D.F., Mexico*

^b*Instituto de Ecología, Universidad Nacional Autónoma de México, México 01000, D.F., Mexico*

Abstract

A new method for distinguishing deterministic chaos from random noise in very short time series is presented. It is based on the scaling properties of the fluctuations present in the first-difference series generated by simple non-linear models widely used in population dynamics. © 1998 Elsevier Science B.V. All rights reserved.

1. Introduction

During the mid 1970s, it became clear that a number of simple mathematical models used in the study of population dynamics often exhibit complex dynamical behaviour in the form of deterministic chaos [1,2]. Since then, the number of techniques available for the study and proper characterisation of chaos has grown considerably. Such techniques include algorithms for measuring invariant quantities such as the divergence of trajectories in the phase space [3,4] or the fractal dimension of the attractor sets [5,6]. However, due to fundamental constraints related to the size of the data [7], these techniques are of limited use when applied to real situations where observational time series are typically very short as is the case of real population dynamics [8]. Because of this, theoretical ecologists have repeatedly used ad hoc models that are parametrized with experimental data. If such models turn out to be chaotic, then it is suspected that the systems under study may also exhibit chaos [9–12].

Another approach was recently discussed by Ikeguchi and Aihara [13] who introduced an innovative method for distinguishing deterministic chaos from coloured noise. Their method is based in the fact that the values of the correlation coefficients calculated between actual and predicted time series and between first-difference actual

* Corresponding author. Tel.: 525 622 5014; fax: +525 622 5015; e-mail: miro@servidor.unam.mx.

and predicted time series show characteristic differences that can distinguish between these two dynamical behaviours. Here we describe an alternative approach based on the scaling properties of first-difference series that is particularly useful for distinguishing deterministic chaos from noise in very short time series. We name this method the First-Difference Scaling Method.

2. First-Difference Scaling Method

The study of the scaling properties of fluctuating processes has increasingly become important in the last decades, specially after the discovery that a range of natural phenomena share the universal property of power law scaling. This is particularly notorious in those systems that are poised in or near critical states [14]. We are interested in the way first-difference temporal fluctuations generated by simple 1D maps scale. The first-difference series (FDS) X_{FD} of a given temporal series $X = \{X_i, \dots, X_n\}$ is defined as $X_{FD} = \|X_i - X_{i+1}\| \geq 0$. This difference series conveys information on the absolute size of the fluctuations.

The method is as follows: two graphs are plotted in such a way that, in the first, the number of fluctuations of a given size are depicted versus the size of the fluctuation using linear axis. The second graph is a log–log transformation of the first. The correlation coefficients of the linear fitting on the linear-axis graph and the power fitting on the log–log axis graph are calculated as standard correlation coefficients $C_L = r^2$ and $C_P = r_{\log}^2$ respectively, where r is given by

$$r = \frac{n(\sum x_i y_i) - (\sum x_i \sum y_i)}{\sqrt{n \sum x_i^2 - (\sum x_i)^2} \sqrt{n \sum y_i^2 - (\sum y_i)^2}},$$

r_{\log}^2 is the coefficient calculated over the log transformed x – y variables that represent the size of the fluctuation and the number of fluctuations, respectively. We will concentrate on the values of the correlation coefficients rather than on the values of the exponents. The reason for this will become clear later.

Both C_L and C_P are related by means of a non-linear transformation. Despite this fact, we will use them as independent variables for visualisation purposes. It turns out that deterministic chaos and noise occupy distinctive regions when C_L and C_P are plotted together in what we call the “correlation space”. More interestingly is the fact that this characteristic behaviour holds even for very short time series. The method just described would be exemplified below when exploring a well-known chaotic simple model.

3. Deterministic chaos and white noise

The existence of deterministic chaos in simple models of population dynamics was first noted in the 1D logistic map [1,2]:

$$X_{n+1} = \mu X_n (1 - X_n).$$

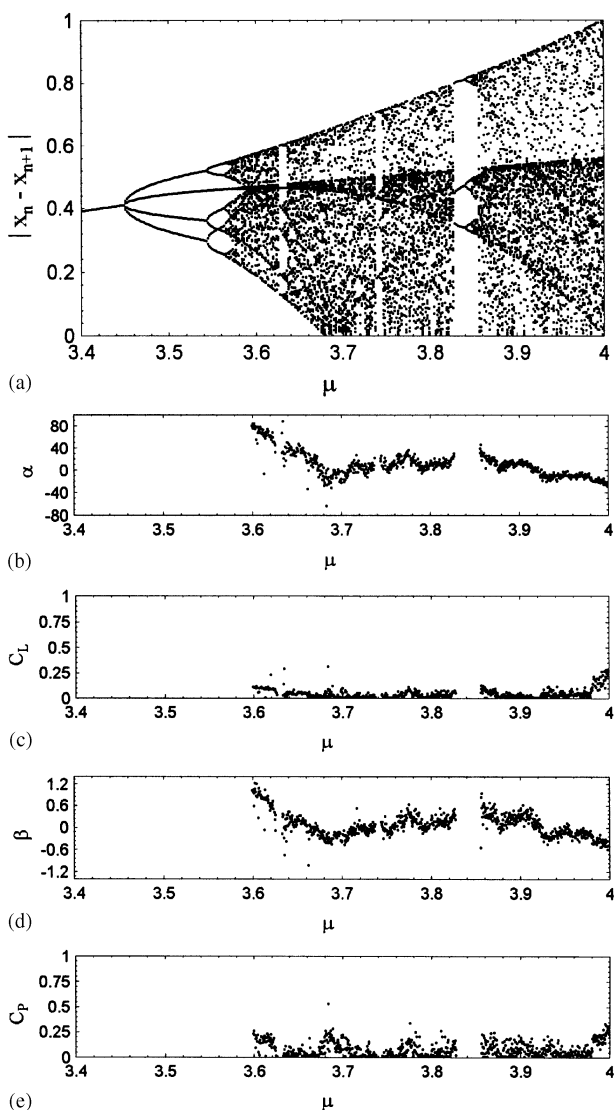


Fig. 1. (a) Shows the bifurcation diagram for the FDS in the logistic map. 10^3 partitions were generated uniformly distributed in the interval $[3.6, 4]$. For each value of μ , a series of length 10^3 was generated after discarding a transient 10^4 long. (b) and (c) A graph was built containing the number of fluctuations versus the size of the fluctuation, then a linear fitting was performed giving the scaling coefficient α and the correlation coefficient C_L . Notice that the values of C_L are typically very low. (d) and (e) The same fitting exercise described above was performed on a log–log transformed graph, then the scaling exponent β and the correlation coefficient C_P were calculated. The values of C_P are very low as in the linear fitting. In all cases $X_0 = 0.1$. The histograms containing the number of fluctuations were calculated with 20 classes of fluctuation sizes and were considered as valid only those containing more or equal than 10 non-empty classes (this eliminates the periodic windows).

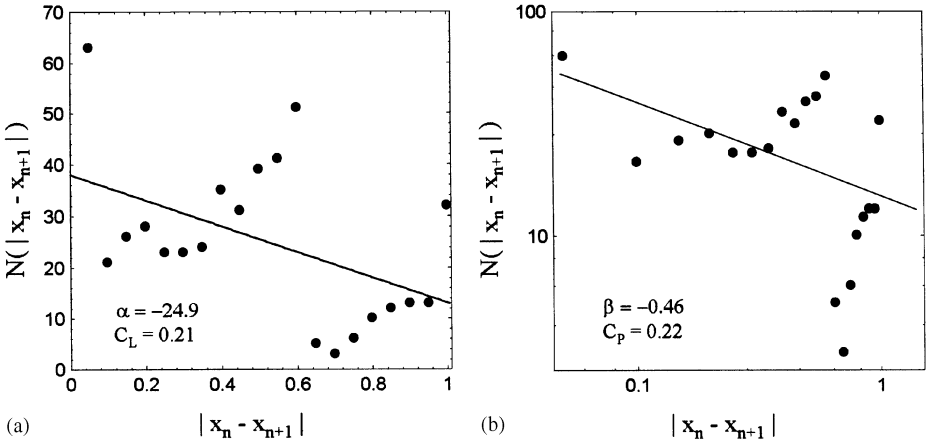


Fig. 2. (a) Linear and (b) power fitting for a FDS generated by the logistic map when $\mu = 4.0$. Notice how the lines representing the best fit do not adjust to the data, giving very low values for the respective correlation coefficients. This particular form of the histograms is typical of all the period-doubling simple maps we explored in this paper.

This map develops chaos by the period-doubling route for values of the bifurcation parameter μ between 3.57 and 4.0. In this interval, a number of FDS were generated and the scaling exponents and correlation coefficients calculated. Fig. 1a shows the bifurcation diagram of these FDS for reference purposes. Fig. 1b–e show the behaviour of the scaling exponents α and β and the coefficients C_L and C_P for the linear and the power fitting, respectively. The logistic map does not fit well into any of these scaling models and this explains the low values of C_L and C_P . In order to see in detail how the FDS of the logistic map scales, the graph containing the number of fluctuations versus the size of the fluctuation is plotted in Fig. 2, for the linear and power fittings.

A similar analysis was performed on random data (Figs. 3 and 4). In this case, first-difference series of white noise uniformly distributed in the interval $[0, 1]$ produced high values of C_L and mid values for C_P . This is, indeed, the fundamental difference in the scaling behaviour that allows distinction between random noise and deterministic chaos. The FDS of random noise scales linearly while deterministic chaos does not fit well into any of both fitting models.

The difference in the scaling behaviour of the FDS of deterministic chaos and random noise is better appreciated when the coefficients C_L and C_P are plotted in the correlation space, that is C_L versus C_P as is shown in Fig. 5. The same data depicted in Figs. 2 and 3 is now shown on the correlation space for the case of four different data lengths. The idea is to see how effectively the method discriminates between deterministic chaos and white noise as the data size is varied. For data 1000 long (Fig. 5d), both data sets are confined into specific disjoint regions of the correlation space, as also happens for shorter sets 500 points long (Fig. 5c). For even shorter data sets of 100 points long

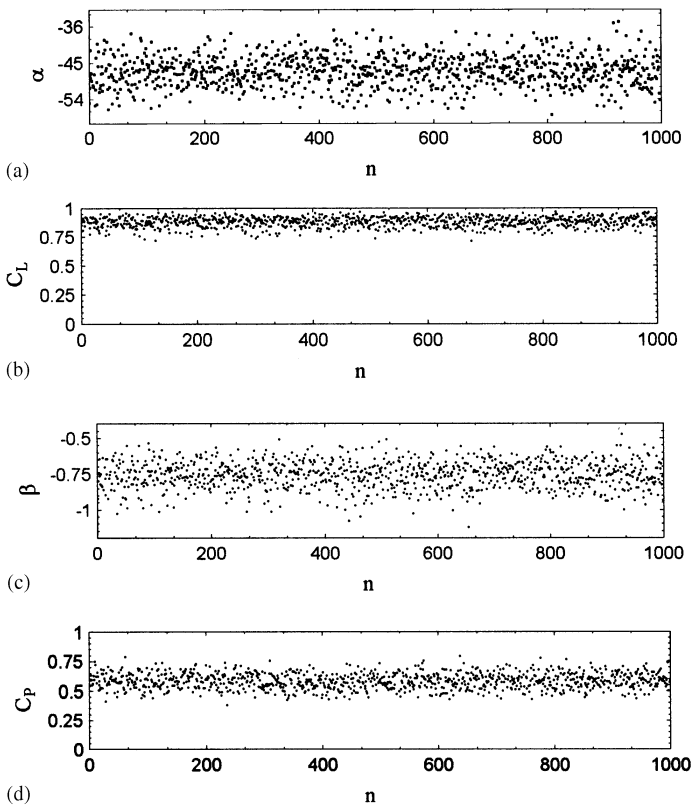


Fig. 3. (a)–(d) Scaling exponents and correlation coefficients for 10^3 uniformly distributed random noise first-difference series 10^3 points long each. Notice that C_L , in contrast to deterministic chaos, takes values close to 1.0 indicating good linear fitting.

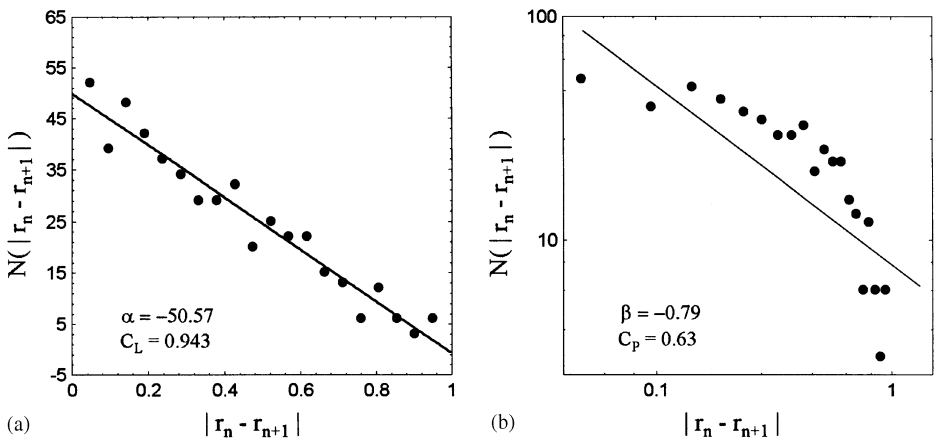


Fig. 4. (a) Linear and (b) power fitting for a random noise FDS. Notice how the line representing the best fit does adjust to the data in the linear case. The series contained 10^3 data.

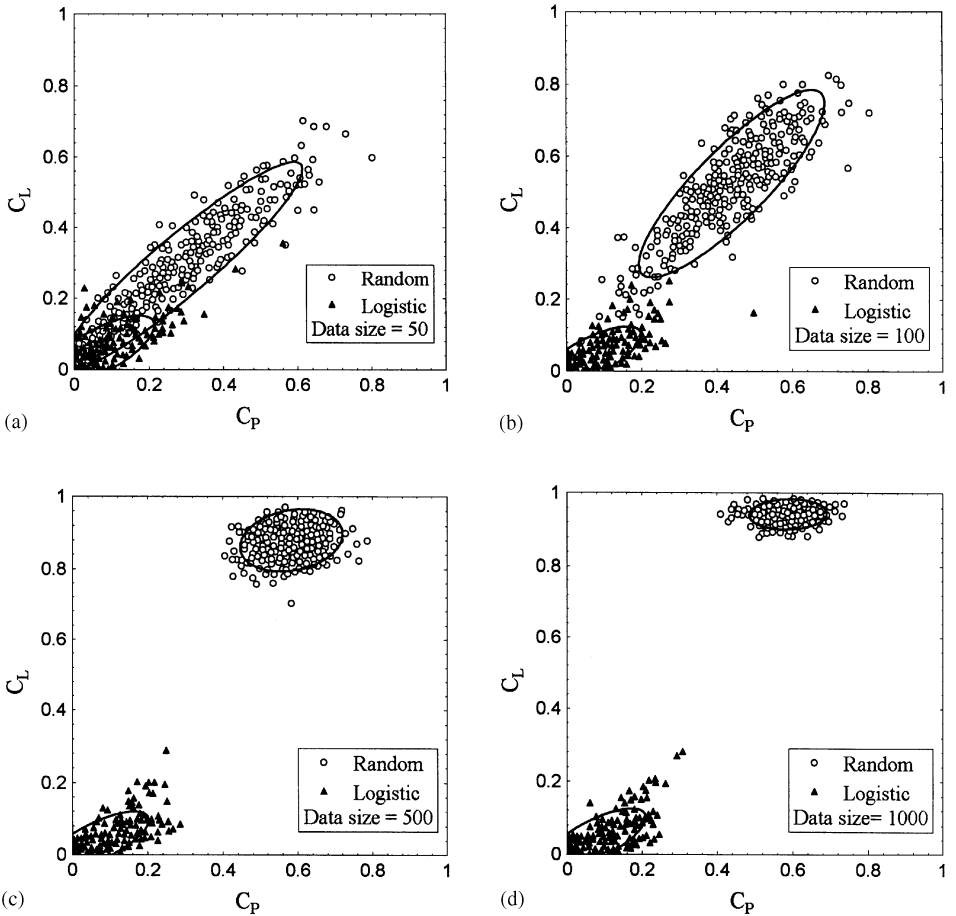


Fig. 5. Chaotic and white noise first-difference series are plotted together in the correlation space as a function of the data length. (a) 50, (b) 100, (c) 500 and (d) 1000 points long. Notice how, even for very short time series, the areas occupied by each data set are clearly distinguishable. The ellipses represent the area containing 95% of the data. The ellipse is calculated as follows. A linear regression is applied to the cloud of data in such a way that the direction of the line fitted is taken as the major axis of the ellipse. A normal distribution was then calculated where the distribution parameter was the confidence limit or the percentage of data explained by such normal distribution.

(Fig. 5b), the areas of the correlation space occupied by each data set are not longer disjoint but it is still possible to differentiate them very well as is also true for very short time series of only 50 points long (Fig. 5a).

So far, we have analysed with this method one of the most simple and well-known population models that exhibits chaos. In the following section other models will be explored as well.

4. Other chaotic models

Other simple 1D chaotic maps that are commonly used in population modelling include [15]:

The Ricker map [15]:

$$X_{n+1} = X_n \exp[\mu(1 - X_n)].$$

The Hassell map [16]:

$$X_{n+1} = \mu X_n [1 + X_n]^{-\beta}.$$

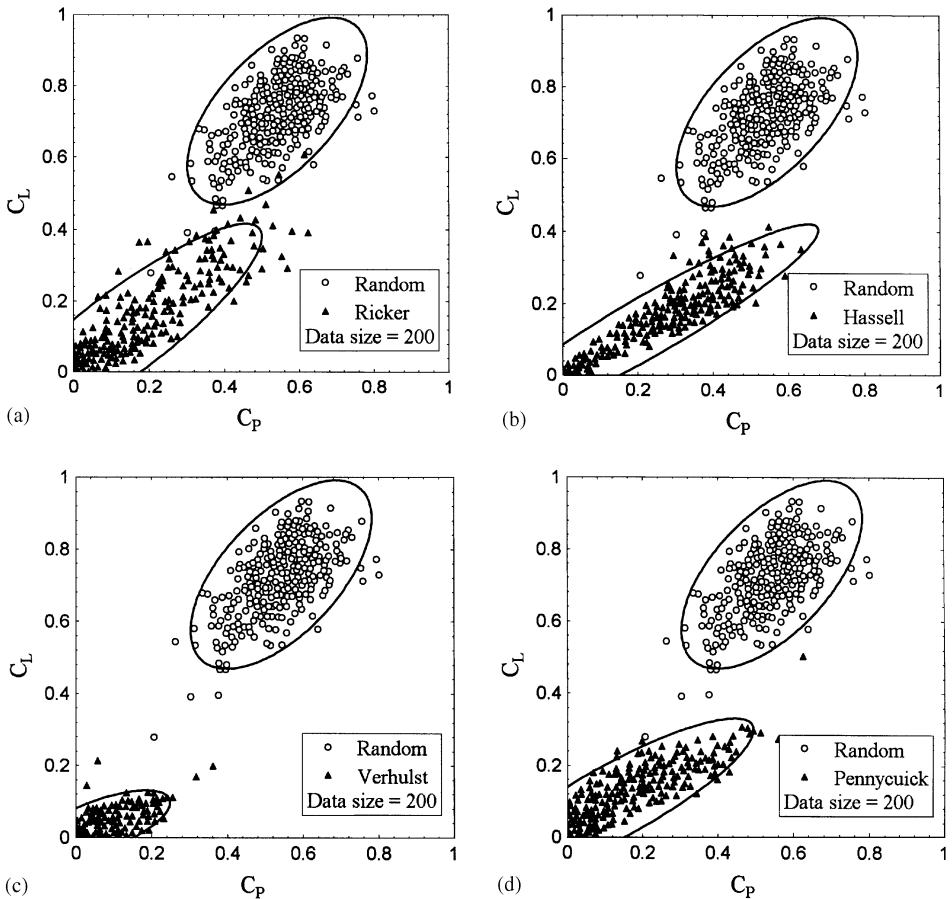


Fig. 6. Correlation space for some well-known maps commonly used in population modelling. (a) Ricker $\mu \in [2.69, 4.0]$, (b) Hassell $\mu \in [65, 140]$, $\beta = 10$, (c) Verhulst $\mu \in [2.6, 2.8]$ and (d) Pennycuik $\mu \in [10, 12]$, $a = 0.1$, $b = 0.1$. 10^3 partitions for the bifurcation parameter μ were calculated in the interval shown, time series are 200 points long. In all cases a transient 10^4 points long was discarded and $X_0 = 0.1$. The ellipses represent the area containing 95% of the data.

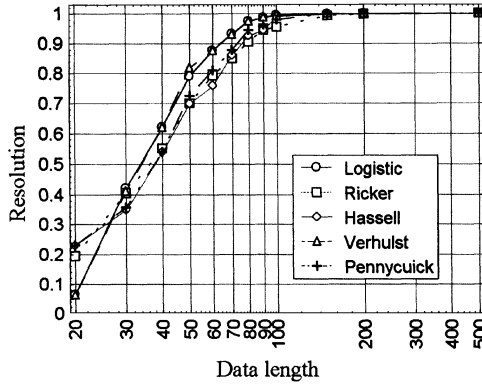


Fig. 7. Resolving power of the method. The resolution probability is plotted versus data size for the five maps discussed. The resolution probability is estimated as the confidence limit of the maximum ellipse that can be drawn on each over the data (chaos and noise) without having these ellipses intersected. All map parameters as in Fig. 6.

The Verhulst map [17]:

$$X_{n+1} = X_n[1 + \mu(1 - X_n)].$$

The Pennycuik map [18]:

$$X_{n+1} = \mu X_n / (1 + \exp[-b(1 - X_n/a)]).$$

All models are 1D single-humped period-doubling maps sharing the same FDS scaling properties of the logistic map as is shown in Fig. 6. The Ricker map was explored for different data sizes (*a*). We present the correlation space for 10^3 first-difference series 200 point long each (the ellipses represent the area where 99.5% of the data are confined). The same analysis was done for the Hassell (*b*), Verhulst (*c*) and Pennycuik maps (*d*). In all the cases, deterministic chaos and white noise are well distinguishable despite the short length of the data.

Finally, Fig. 7 shows the resolving capability of the first-difference scaling method for distinguishing deterministic chaos from white noise, for each of the maps studied and for different data sizes. The Resolution was estimated as the area of the ellipses that can accommodate the maximum percentage of data without having the areas intersected. The method is very robust for all the maps since they all follow a common pattern. The method is also very precise since the resolving power for short series is good enough. Take for example series 100 points long, the method has a resolution of about 0.999 for this data size in all the models studied.

5. Discussion

It was shown that the scaling of first-difference fluctuations of time series convey information that can distinguish between deterministic chaos generated by simple maps

and white noise, even for very short time series. There are many open lines for future research: preliminary results show that other routes to chaos could also be distinguished from period-doubling chaos. The method also seems to be helpful in distinguish between coloured noise such as $1/f$, Brownian and white noise. A sound theoretical basis for this method remains for the future.

Acknowledgements

We are grateful to P. Miramontes for stimulating discussion. It is also a pleasure to thank Pejman Rohani for his perceptive comments on this paper and T. Ikeguchi for providing a copy of his paper's abstract. This work was partly supported by a DGAPA-UNAM fellowship (IN 108496) and a CONACYT grant (3280P-E9607) to O.M. No part of this research was supported by military-related funds.

References

- [1] R.M. May, *Science* 186 (1974) 645.
- [2] R.M. May, *Nature* 261 (1976) 459.
- [3] A. Wolf, J.B. Swift, H.L. Swinney, J.A. Vastano, *Physica D* 16 (1985) 285.
- [4] K. Briggs, *Phys. Lett. A* 151 (1990) 27.
- [5] P. Grassberger, I. Procaccia, *Phys. Rev. Lett.* 50 (1983) 346.
- [6] J. Theiller, *J. Opt. Soc. Am. A* 7 (1990) 1055.
- [7] J.P. Eckmann, D. Ruelle, *Physica D* 56 (1992) 185.
- [8] S. Ellner, P. Turchin, *Am. Nat.* 145 (1995) 343.
- [9] M.P. Hassell, J.H. Lawton, R.M. May, *J. Anim. Ecol.* 45 (1976) 471.
- [10] D. Tilman, D. Wedin, *Nature* 353 (1991) 653.
- [11] R.F. Costantino, J.M. Cushing, B. Dennis, R.A. Desharnais, *Nature* 375 (1995) 227.
- [12] P. Rohani, O. Miramontes, *J. Anim. Ecol.* 65 (1996) 847.
- [13] T. Ikeguchi, K. Aihara, *Phys. Rev. E* 55 (1997) 2530.
- [14] P. Bak, C. Tang, K. Wiesenfeld, *Phys. Rev. A* 38 (1988) 364.
- [15] W.E. Ricker, *J. Fish. Res. Bd Can.* 11 (1954) 559.
- [16] M.P. Hassell, *J. Anim. Ecol.* 44 (1974) 283.
- [17] R.M. May, G. Oster, *Am. Nat.* 110 (1976) 573.
- [18] C.J. Pennycuik, R.M. Compton, L. Beckingham, *J. Theor. Biol.* 18 (1968) 316.